REPORT DOCUMENTATION PAGE

Form Approved OMB No. 0704-0188

1. REPORT DATE (DD-MM-YYYY)	2. REPORT TYPE	3. DATES COVERED (From - To)
02/23/2004	Journal	

4. TITLE AND SUBTITLE

Gas Phase Structural Characterization of Polyhedral Oligomeric Silsesquioxanes (POSS) with Styryl and Epoxy Phenyl Capping Agents

5a. CONTRACT NUMBER
F04611-99-C-0025

5b. GRANT NUMBER

5c. PROGRAM ELEMENT NUMBER

6. AUTHOR(S)

Timothy S. Haddad, Erin shammel Baker, Jennifer Gidden, Stanley E. Anderson, Michael T. Bowers

5d. PROJECT NUMBER
2303

5e. TASK NUMBER
M1A3

5f. WORK UNIT NUMBER

7. PERFORMING ORGANIZATION NAME(S) AND ADDRESS(ES)

ERC Incorporated
555 Sparkman Drive
Huntsville, AL 35816-0000

8. PERFORMING ORGANIZATION REPORT NUMBER

9. SPONSORING / MONITORING AGENCY NAME(S) AND ADDRESS(ES)

Air Force Research Laboratory (AFMC)
AFRL/PRS
5 Pollux Drive
Edwards AFB, CA 93524-7048

10. SPONSOR/MONITOR'S ACRONYM(S)

11. SPONSOR/MONITOR'S NUMBER(S)
AFRL-PR-ED-TP-2004-045

12. DISTRIBUTION / AVAILABILITY STATEMENT

Approved for public release; distribution unlimited.

13. SUPPLEMENTARY NOTES
Journal – Nano Letters

14. ABSTRACT

15. SUBJECT TERMS

16. SECURITY CLASSIFICATION OF:			17. LIMITATION OF ABSTRACT	18. NUMBER OF PAGES	19a. NAME OF RESPONSIBLE PERSON
a. REPORT	b. ABSTRACT	c. THIS PAGE			Linda Talon
Unclassified	Unclassified	Unclassified	A	26	19b. TELEPHONE NUMBER (include area code) (661) 275-5283

Gas Phase Structural Characterization of Polyhedral Oligomeric Silsesquioxanes (POSS) with Styryl and Epoxy Phenyl Capping Agents

*Erin Shammel Baker, Jennifer Gidden, Stanley E. Anderson†, Timothy S. Haddad‡, and Michael T. Bowers**

Department of Chemistry & Biochemistry, University of California, Santa Barbara CA 93106

bowers@chem.ucsb.edu

RECEIVED DATE (to be automatically inserted after your manuscript is accepted if required according to the journal that you are submitting your paper to)

† Department of Chemistry, Westmont College, Santa Barbara, CA 93108

‡ ERC Inc., Air Force Research Laboratory, 10 East Saturn Boulevard, Building 8451, Edwards AFB, CA 93524-7680.

modeling methods were used to examine the gas phase structures of sodiated POSS capped with styryl and epoxy phenyl substituents ($Na^+Sty_xEp_{8-x}T_8$). Results were obtained for x = 5-7 and indicated that three distinct isomers with different collision cross-sections were present for each value of x. Theoretical modeling also yielded three different families of structures for each POSS system and their calculated cross-sections agreed very well with experimental values (<1% difference). For $Na^+Sty_7EpT_8$, the three families differ in the number of "paired" Sty groups. For $Na^+Sty_6Ep_2T_8$ and $Na^+Sty_5Ep_3T_8$, the three isomers correspond to the three different ways the Ep groups can be positioned on the POSS cage.

Inorganic-organic materials research is a rich and fast-developing area of nanotechnology that promises to provide a wide variety of commercial applications. Nanocomposites, derived from distinctly dissimilar inorganic and organic subunits combined on a nanometer length scale, can have extraordinary properties. Their macroscopic properties are usually superior to those found for conventional microscale composites due to the morphology and interfacial characteristics derived from mixing dissimilar materials on such tiny length scales. By adding inorganic components into organic polymers, mechanical[1], thermal[2-5], electrical[6] and magnetic[7] properties are altered from those of pure organic polymers. These property advances have caused a surge of interest in nanocomposite synthesis and analysis with the promise of new applications in many fields, including non-linear optics, sensors, and nanowires[8, 9].

Polyhedral oligomeric silsesquioxanes (POSS) are one type of material capable of forming nanocomposites[10, 11]. POSS cages are nanoscopic in size and composed of a rigid three-dimensional Si-O framework of the form $(RSiO_{3/2})_n$, where R is typically an alkyl or aryl organic group. The properties of POSS are unique since one or more of the organic groups can be made reactive for polymerization, while the remaining unreactive groups solubilize the inorganic core and allow for control over the interfacial interactions occurring between POSS and the polymer matrix[12-14]. POSS units can be added to virtually all polymer types either by blending[15], grafting[16-18] or copolymerization reactions[19-24]. By

incorporating the rigid Si-O cage into polymers, property enhancements such as increased thermal stability, reduced flammability, reduced viscosity and lowered density have been observed[11-26]. These property enhancements make POSS compounds of great interest to further improve high performance polymers and to develop multifunctional materials. However, it is essential to understand the conformation of the POSS monomers before they are incorporated into polymer systems in order to predict the compatibility and solubility[27] of the monomers with the polymer systems.

In order to study different POSS conformers, a technique has been developed in our group to incorporate both mass spectrometry and ion mobility[28, 29] into the analysis so ions can be studied based on their mass and conformational size. With the help of matrix assisted laser desorption/ionization (MALDI)[30] and time of flight (TOF) mass spectrometry, ions in a sample can be identified by their mass and their relative abundance can be determined. Ion mobility then allows the ion of interest to be mass-selected and analyzed as a function of time while it drifts through a buffer gas under the influence of a uniform, weak electric field. Structural analysis can be performed on the ion depending on the amount of time it takes the ion to drift through the buffer gas and arrive at the detector.

In this paper we report on the application of ion mobility to the structural analysis of POSS monomers cationized by sodium with a mixture of styryl (Sty) and epoxy phenyl (Ep) capping substituents. The Ep group differs from the Sty capping substituent only by the epoxidation of the vinyl linkage, which connects the Sty group to the Si-O cage.

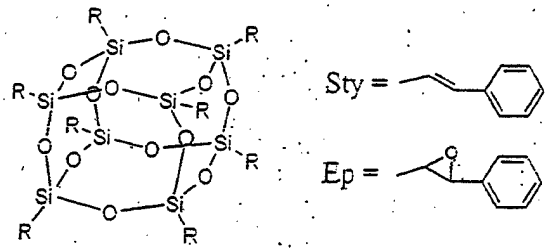

Mixed $Sty_xEp_{8-x}T_8$ POSS systems were synthesized for incorporation into linear polymers and network resins. Sty_8T_8 can be blended with various organic polymers. However, with the epoxidation of the Sty groups' vinyl linkages to create Ep groups, it is possible to crosslink the POSS into a cured

The reactions of the Ep capping substituent with polyamines forms amino alcohols that can further react with another Ep group to make a network crosslink[31, 32]. Also, having both Sty and Ep groups on the exterior of the POSS cage has allowed for the polymerization of the mixed $Sty_xEp_{8-x}T_8$ POSS systems into vinyl ester, phenolic, epoxy, and dicyclopentadiene (DCPD) resins[27]. The ability to polymerize so many different resins has proved that having many functionalized substituents is essential in developing improved nanocomposites. Thus, in order to develop better nanocomposites, it is essential to fully understand how the $Sty_xEp_{8-x}T_8$ POSS systems are interacting within the resins, and therefore it is important to first identify the structure and interactions occurring within the monomers. Since ion mobility can detect conformers based on different sizes, it is a vital tool in understanding the $Sty_xEp_{8-x}T_8$ POSS monomer structures.

A MALDI-TOF mass spectrum of the $Sty_xEp_{8-x}T_8$ POSS system doped with NaI is shown in Figure 1. Only ions for $x = 4$ to 8 are observed in the mass spectrum. Ion mobility results for $Na^+Sty_8T_8$ have been published[33] so this system will not be discussed here. The abundance of $Na^+Sty_4Ep_4T_8$ was too small for ion mobility analysis, so only data for the analysis of $Na^+Sty_7EpT_8$, $Na^+Sty_6Ep_2T_8$ and $Na^+Sty_5Ep_3T_8$ will be discussed. For the ion mobility experiments, the appropriate $Na^+Sty_xEp_{8-x}T_8$ ions are gently injected into the drift cell and their arrival time distributions (ATDs) collected. Typical ATDs are shown in Figure 2 for sodiated Sty_7EpT_8, $Sty_6Ep_2T_8$ and $Sty_5Ep_3T_8$.

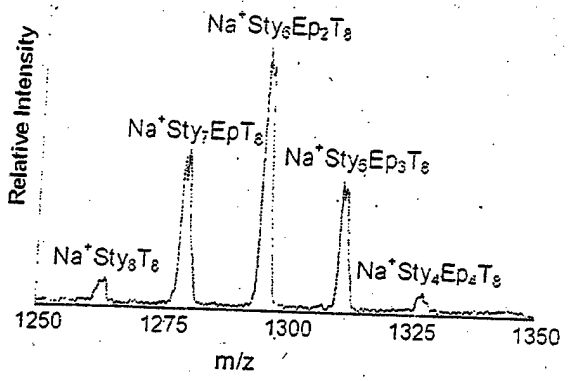

Figure 1. MALDI-TOF mass spectrum of the sodiated $Sty_xEp_{8-x}T_8$ sample.

Na^+ Sty_7EpT_8. Three resolvable features are apparent in the $Na^+Sty_7EpT_8$ ATD indicating three distinct conformers with different mobilities exist. In order to better analyze these features, the temperature of the drift cell was decreased from 300K to 120K to slow down any possible isomerization and to increase the resolution of the ATD peaks[34-36]. As the temperature was lowered, no new peaks were detected but the resolution of the ATDs increased. Therefore, Figure 2 only illustrates the high resolution ATDs at 120K. The collision cross-sections of each ATD peak are extracted at 300K using equations 1 and 2 (in the supporting material) and these values and the relative abundance of each peak are listed in Table 1. The shape of the ATD peaks did not change as a function of injection energy (300-500eV) so the relative intensities should be accurate representations of the abundance of each conformer exiting the MALDI source.

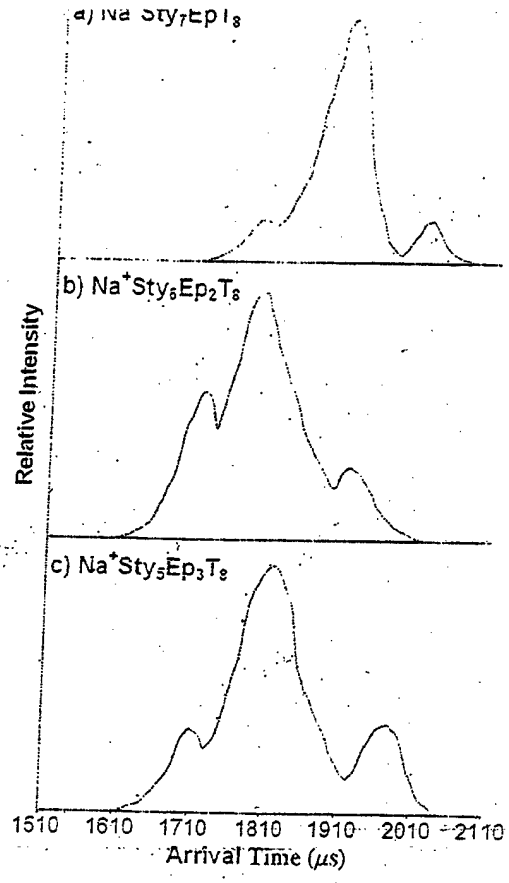

Figure 2. Arrival time distributions (ATDs) of a) $Na^+Sty_7EpT_8$ b) $Na^+Sty_6Ep_2T_8$ and c) $Na^+Sty_5Ep_3T_8$ obtained at a drift cell temperature of 120K for best resolution. The multiple peaks in the ATDs represent multiple conformations of the ion that have different collision cross-sections.

Table 1. Collision Cross-Sections (Å^2) for $Na^+Sty_7EpT_8$, $Na^+Sty_6Ep_2T_8$ and $Na^+Sty_5Ep_3T_8$

Name	Experiment	Theory	% Abundance[j]
	319	320[a]	13%
$Na^+Sty_7EpT_8$	323	324[b]	74%
	327	328[c]	13%
	315	314[d]	22%
$Na^+Sty_6Ep_2T_8$	319	319[e]	66%
	324	322[f]	12%
	314	314[g]	17%
$Na^+Sty_5Ep_3T_8$	319	319[h]	66%
	327	326[i]	17%

Calculated average cross-sections for a) "3 pair" family, b) "2 pair" family, c) "1 pair" family, d) 2 Ep on adjacent corners, e) 2 Ep face-diagonal, f) 2 Ep on opposite corners, g) 3 Ep on adjacent corners, h) 2 Ep on adjacent corners, i) Ep on opposite corners and j) from relative intensities of ATD peaks

Theoretical structures of $Na^+Sty_7EpT_8$ are generated by placing one Ep group on a corner of the Si_8O_{12} cube and Sty groups on the remaining seven corners. Using the methods described in the theoretical section, a simulated annealing cycle is used to produce 100 low-energy structures for $Na^+Sty_7EpT_8$, $Na^+Sty_6Ep_2T_8$ and $Na^+Sty_5Ep_3T_8$. After the structures are generated, their angle averaged collision cross-sections are calculated using a previously developed projection model described in the supporting material. Cross-sections and energies are then plotted for each theoretical structure to help identify the ions observed in the ATDs. The scatter plot observed for $Na^+Sty_7EpT_8$ is illustrated in Figure 3.

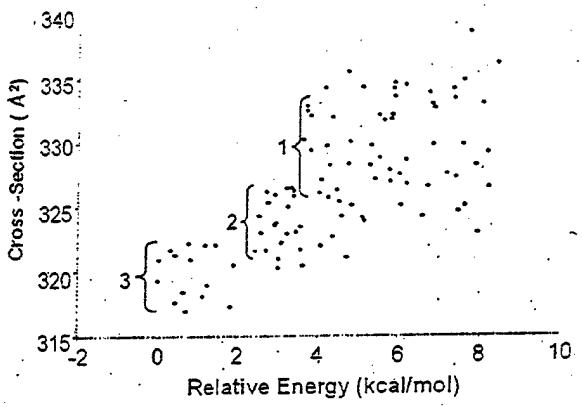

Figure 3. Plot of cross-section vs. energy for $Na^+Sty_7EpT_8$. Each point represents one theoretical structure generated by the simulated annealing method. Three families of structures are predicted that differ in the number of paired Sty groups (see Figure 4).

The scatter plot shows three distinct families of conformers (labeled "3", "2" and "1" in Figure 3) that differ in energy and cross-section. Examples of each family are shown in Figure 4. In each family, the Ep and the Sty groups extend away from the Si-O cage and the Na^+ ion coordinates to one oxygen on the cage and the oxygen associated with the epoxy group. The phenyl group of Ep interacts with a phenyl group of a neighboring Sty substituent in a "tilted T"[37] arrangement. In this arrangement, the Ep phenyl is 5Å away from and approximately perpendicular to the Sty phenyl group (see inset in Figure 4).

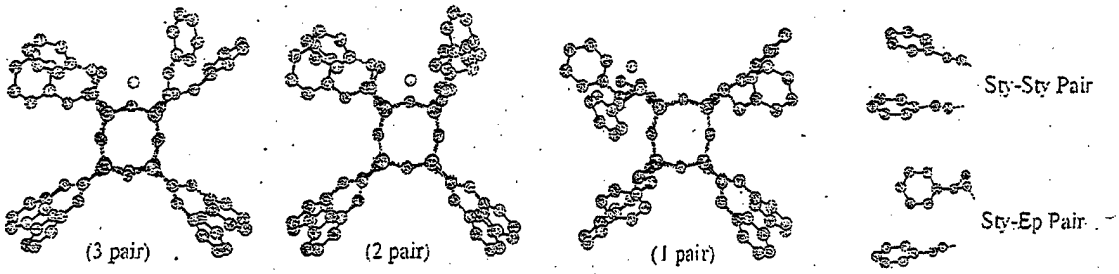

Figure 4. The three distinct conformers calculated for $Na^+Sty_7EpT_8$. Sty-Sty pairs are colored blue, carbon atoms are gray, silicon is green, oxygen atoms are red, and sodium is yellow (hydrogen atoms have been omitted for clarity). Sty-Ep "pairs" have a "tilted T" conformation and Sty-Sty "pairs" have a "displaced parallel" conformation (shown in inset).

The families of structures differ in how the remaining Sty groups interact with each other. Along with the Sty-Ep "pair", two nearest-neighbor Sty groups can form pairs in which the two phenyl groups are parallel to each other (not stacked) and displaced by 5Å. These Sty-Sty pairs are shown in blue in Figure 4. "Unpaired" Sty groups maintain a 10Å distance between phenyl groups. No more than two phenyl groups form a given pair and each pair does not interact with any other Sty groups. Since six Sty groups are available for pairing (there is always 1 Sty-Ep pair), one, two or three Sty-Sty pairs can form. This Sty-Sty pairing was also observed in the structures of $Na^+Sty_8T_8$[33].

In the lowest energy family of structures, all 8 Sty/Ep substituents are paired. The Ep group pairs with a Sty group to form a "tilted T" pair while the remaining 6 Sty groups form 3 Sty-Sty pairs. Consequently, this "3-pair" family has the smallest cross-section (320Å^2). The second family of structures, which is ~3 kcal/mol higher in energy and 4Å^2 larger in cross-section, has 2 Sty-Sty pairs along with the Sty-Ep pair. The two unpaired Sty groups are nearest neighbors but remain 10Å from each other and the other pairs. The third family of structures, which is ~4 kcal/mol higher in energy and 8Å^2 larger in cross-section than the "3-pair" family, has 1 Sty-Sty pair and 1 Sty-Ep pair.

The calculated cross-section of each family of $Na^+Sty_7EpT_8$ structures is compared to experimental values in Table 1. The cross-section from the shortest-time ATD peak (see Figure 2a) agrees very well with the cross-section for the "3 pair" family. The cross-section from the intermediate ATD peak, which is the most abundant peak, matches the cross-section of the family with 2 Sty-Sty pairs, and the cross-section from the longest-time ATD peak corresponds with that of the 1 Sty-Sty pair family.

$Na^+Sty_6Ep_2T_8$. A typical 120K ATD for sodiated $Sty_6Ep_2T_8$ is shown in Figure 2b. As with $Na^+Sty_7EpT_8$, three resolvable features appear in the ATD for $Na^+Sty_6Ep_2T_8$ that do not interconvert or change in intensity with injection energy. The experimental cross-section and relative abundance of each peak is listed in Table 1.

With more than one Ep group present on the T_8 cage, several isomers are possible for $Sty_6Ep_2T_8$ based on the relative positions of the Ep groups. The 2 Ep groups can either be placed on adjacent corners of the Si-O cage, on opposite corners on the same face of the cage or on opposite corners of the entire cage. The scatter plots of cross-section versus energy for the 100 theoretical structures predicted for each isomer is shown in Figure 5. In each case, only one family of conformers is predicted and the lowest-energy structures displayed in Figure 6.

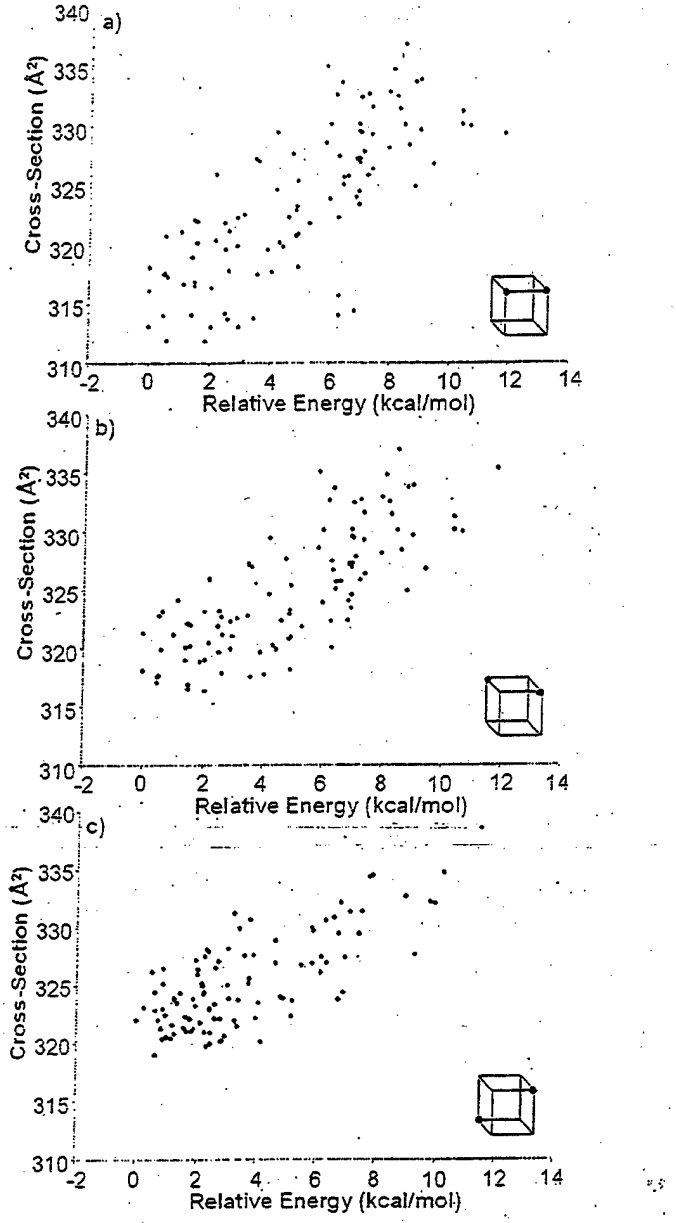

Figure 5. Plots of cross-section vs. energy for the three geometric isomers of $Na^+Sty_6Ep_2T_8$ with the 2 Ep groups a) on adjacent corners, b) face-diagonal to each other and c) on opposite corners of the Si-O cage. One low-energy family of structures is predicted for each isomer.

The isomer with the Ep groups on adjacent corners of the Si-O cage has the smallest average cross-section ($314 \pm 4 Å^2$) of the three isomers. The Na^+ ion lies between the two Ep groups and coordinates to one oxygen on the Si-O cage and the two oxygens associated with the epoxy groups. All eight of the

Sty and Ep groups form 7 pairs. Four of the six Sty groups form 2 Sty-Sty pairs and the other two Sty groups interact with the two Ep groups to form 2 Sty-Ep pairs. As in the $Na^+Sty_7EpT_8$ case, only two Sty or Ep groups are involved in a given pair and none of the pairs interact with any other pair. The two Ep groups do not form an Ep-Ep pair due to the nature of the Na^+-O interactions. In order for the two epoxy oxygens to be in a good position to coordinate to Na^+, the two phenyl groups must rotate away from each other, thus preventing an Ep-Ep pair from forming. However, this rotation also puts the Ep phenyl groups in a good position to form a "tilted T" pair with a neighboring Sty group.

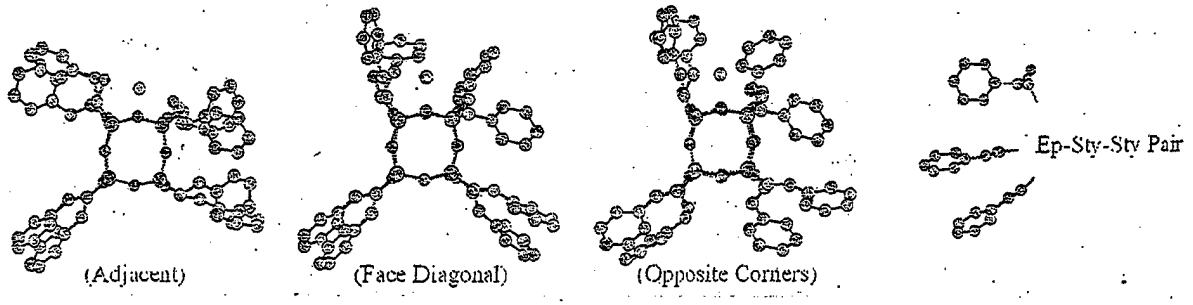

Figure 6. The lowest-energy structures calculated for the three isomers of $Na^+Sty_6Ep_2T_8$. The Ep groups are shown in pink. In the face-diagonal isomer, an Ep group couples to a Sty-Sty pair resulting in an Ep-Sty-Sty trio.

A face-diagonal positioning of the Ep groups leads to a slightly different structure with an average cross-section ($319 \pm 4 Å^2$) that is $5 Å^2$ larger than the isomer with Ep groups on adjacent corners. In this case, Na^+ lies between an Ep and Sty group and coordinates to one oxygen on the Si-O cage, the epoxy oxygen on the Ep group and the vinyl linkage on the Sty group (similar to the Na^+ coordination in $Na^+Sty_7EpT_8$). As with the "adjacent" isomer, four of the six Sty groups in the "face-diagonal" isomer form 2 Sty-Sty pairs. However, only one Sty-Ep pair forms (involving the Sty and Ep groups not coordinated to Na^+). As in the "adjacent" isomer, the Sty and Ep groups coordinated to Na^+ cannot form a pair because the phenyl group on Ep rotates away from the Sty group so that the epoxy oxygen can coordinate to Na^+. However, unlike the "adjacent" isomer in which the two Ep groups paired with

neighboring Sty groups, the Sty group in this isomer is pulled toward the Na^+ ion and cannot pair with any neighboring Sty groups. The Ep group on the other hand, actually interacts with a Sty-Sty "pair" forming an Ep-Sty-Sty trio. This is the first example of more than two Sty or Ep groups being coordinated in a given unit.

The isomer with the Ep groups on opposite corners of the cage has the largest average cross-section ($322 \pm 4 Å^2$) of the three isomers. As in the "face-diagonal" isomer, the Na^+ ion lies between an Ep and Sty group and coordinates to one oxygen on the Si-O cage, one Ep oxygen, and a vinyl group on Sty. In this case, the two Ep groups pair with neighboring Sty groups to form 2 Sty-Ep pairs but only 1 Sty-Sty pair is formed. The Sty group coordinated to Na^+ is unpaired for the same reasons as the unpaired Sty groups in the "face-diagonal" isomer. The remaining unpaired Sty group is on the opposite corner of the Si-O cage. It appears to be simply the "odd man out" as all of its nearest neighbors are paired with other groups. However, this Sty group is in a position to form an Ep-Sty-Sty trio, similar to the one observed in the "face-diagonal" isomer, yet remains unpaired. The reason is that the Sty group is slightly pulled toward the other Ep group (not coordinated to Na^+) and away from the Sty group necessary to form the Ep-Sty-Sty trio.

The calculated cross-section of each $Na^+Sty_6Ep_2T_8$ isomer is compared to experimental values in Table 1. The cross-section from the shortest-time ATD peak (Figure 2b) agrees well with the theoretical value for the isomer with the Ep groups placed on adjacent corners of the Si-O cage. The cross-section from the intermediate ATD peak matches that of the "face-diagonal" isomer and the peak at the longest time in the ATD corresponds to the isomer with Ep groups in opposite corners of the cage. The peak corresponding to the isomer with Ep groups diagonal on the face of the Si-O cage is the most abundant peak in the ATD, indicating that the "face-diagonal" isomer is the most abundant isomer produced in the synthesis.

Na^+ $Sty_5Ep_3T_8$. A typical 120K ATD for $Na^+Sty_5Ep_3T_8$ is shown in Figure 2c. Like the other two Sty/Ep compounds, the ATD for $Na^+Sty_5Ep_3T_8$ has three peaks where the middle peak is the most

intense. The experimental cross-sections and relative abundances derived from the three ATD peaks at 300K are listed in Table 1.

As with $Na^+Sty_6Ep_2T_8$, three isomers are possible for $Na^+Sty_5Ep_3T_8$ depending on the positioning of the Ep groups on the Si-O cage. The 3 Ep groups can be placed on adjacent corners of the Si-O cage, 2 Ep groups can be placed on adjacent corners and the third Ep placed on an opposite corner of the cage, or all 3 Ep groups can be placed on opposite corners of the cage. Plots of cross-section versus energy for the 100 generated structures of each isomer are shown in Figure 7. In each case, only one family of conformers is predicted and the lowest-energy structures for each isomer are displayed in Figure 8.

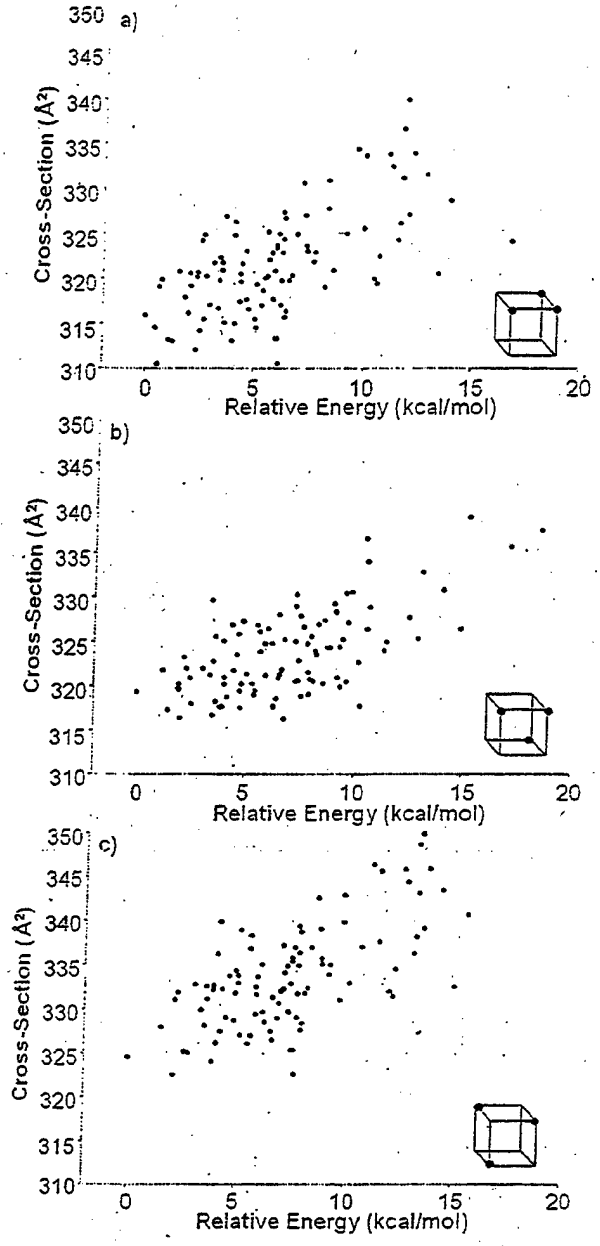

Figure 7. Plots of cross-section vs. energy for $Na^+Sty_5Ep_3T_8$ with a) all 3 Ep groups on adjacent corners, b) 2 Ep groups adjacent and the third on an opposite corner and c) all 3 Ep groups on opposite corners. One family of low-energy structures is predicted for each isomer.

The isomer with all 3 Ep groups on adjacent corners of the Si-O cage (Figure 8a) has the smallest average cross-section ($314 \pm 4 Å^2$) of the three isomers. The Na^+ ion lies between two of the Ep groups and coordinates to one oxygen on the Si-O cage and the two epoxy oxygens on the Ep groups. All of

the Sty and Ep groups are paired. The three Ep groups pair with neighboring Sty groups to form 3 Sty-Ep pairs and the remaining two Sty groups, which are nearest neighbors, form 1 Sty-Sty pair. However, unlike any of the other Sty/Ep systems, two pairs interact with each other in this isomer. Two Sty groups involved in Sty-Ep pairing interact to form a Sty-Sty pair as well (shown in blue in Figure 8a), leading to a more compact structure.

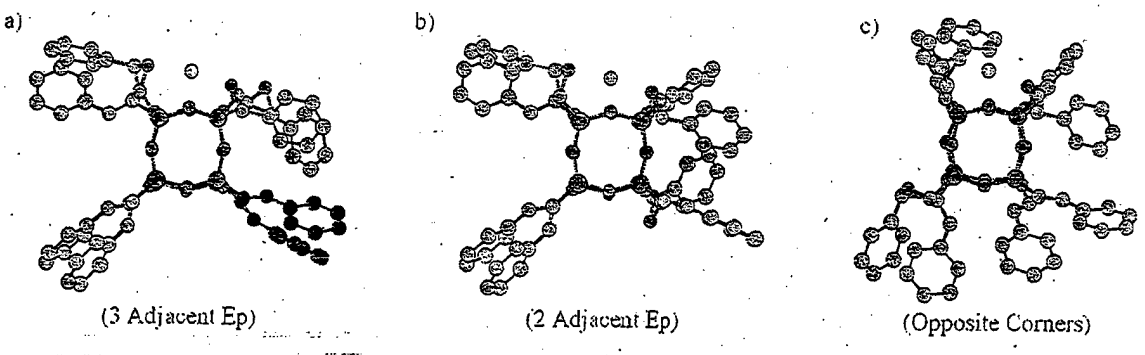

Figure 8. Lowest-energy structures calculated for the three isomers of $Na^+Sty_5Ep_3T_8$. The Ep groups are shown in pink. In the isomer with 3 adjacent Ep groups, two Sty-Ep pairs are paired together by a Sty-Sty interaction. The interacting Sty groups are shown in dark blue.

The isomer with 2 Ep groups on adjacent corners of the Si-O cage and the third Ep on an opposite corner (Figure 8b) has an average cross-section ($319 \pm 4 Å^2$) that is $5 Å^2$ larger than the "3 adjacent" isomer described above. The Na^+ interactions and the Sty/Ep pairing are similar to those observed in the "3 adjacent" isomer. The Na^+ ion coordinates to one oxygen on the Si-O cage and two epoxy oxygens, which results in the formation of 3 Sty-Ep pairs and 1 Sty-Sty pair. The difference, and hence larger cross-section, is that none of the pairs interact with any other pairs.

The isomer with the 3 Ep groups on opposite corners of the Si-O cage (Figure 8c) has the largest average cross-section ($326 \pm 4 Å^2$) of the three isomers. In this case, Na^+ rests between a Sty and Ep

group and coordinates to one oxygen on the Si-O cage, the epoxy oxygen on the Ep group and the vinyl linkage on the Sty group. Only 2 Sty-Ep pairs and 1 Sty-Sty pair are formed in this isomer. As in the "face-diagonal" isomer for $Na^+Sty_6Ep_2T_8$, the Sty group coordinated to Na^+ is not involved in a pair because it is pulled slightly toward the Na^+ ion and away from the neighboring Ep groups. Also like the "face-diagonal" isomer, the remaining unpaired Ep group (which cannot pair with the Sty group coordinated to Na^+) interacts with the Sty-Sty pair to form an Ep-Sty-Sty trio.

Table 1 compares the calculated cross-sections for each $Na^+Sty_5Ep_3T_8$ isomer to those determined from the ATDs (Figure 2c). The peak with the shortest time in the ATD yields a cross-section that agrees very well with the calculated value for the isomer with all 3 Ep groups placed on adjacent corners. The cross-section determined from the middle peak in the ATD matches the value calculated for the isomer with the 2 adjacent Ep groups and the cross-section determined from the longest time peak in the ATD corresponds to the 3 Ep groups on opposite corners of the cage. The middle peak is the most abundant peak in the ATD so the isomer with only 2 Ep groups together is likely the most abundant isomer produced in the synthesis.

Summary. Three related $Na^+Sty_xEp_{8-x}T_8$ POSS cage systems (with x = 5, 6, and 7) have been analyzed using ion mobility experiments and MM/MD modeling. The major findings are as follows:

1) For each system (x = 5, 6, and 7), three families of isomers are found.
2) For x=5 or 6, these families correspond to the different ways the Ep groups can be distributed on the POSS cage. For x=7, the families are associated with pairing of the Sty and Ep capping groups.
3) MM/MD modeling yields 3 families of structures for each value of x, in agreement with experiment. The cross-sections calculated from the low energy structures in each family agree with experiment to within 1% for all 9 systems.

4) The Sty-Sty pairs have their phenyl groups parallel to each other and about 5Å apart. The Sty-Ep pairs have a "tilted T" structure where the planes of the phenyl groups are at a ~90° angle.

5) The distribution of the Ep capping agents on the POSS cage is determined for x=5 and 6. These distributions are similar to statistical predictions but are sufficiently different that the subtle energetics of capping group pairing is probably involved in determining the actual observed distributions.

Acknowledgement. The Air Force Office of Scientific Research under grant F49620-03-1-0046 is gratefully acknowledged.

Supporting Information Available: Details of the experimental procedures and theoretical modeling used for data analysis. This material is available free of charge via the Internet at http://pubs.acs.org.

References

1. Okada, A.; Usuki, A. *Mater. Sci. Eng. C* 1995, *3*, 109.

2. Gilman, J.W. *Appl. Clay Sci.* 1999, *15*, 31.

3. Gilman, J.W.; Jackson, C.L.; Morgan, A.B.; Harris, Jr., R.; Manias, E.; Giannelis, E.P.; Wuthenow, M.; Hilton, D.; Phillips, S.H. *Chem. Mater.* 2000, *12*, 1866.

4. Porter, D.; Metcalfe, E.; Thomas, M.J.K. *Fire Mater.* 2000, *24*, 45.

5. Zanetti, M.; Lomakin, S.; Camino, G. *Macromol. Mater. Eng.* 2000, *279*, 1.

6. Armes, S.P. *Polym. News* 1995, *20*, 233.

7. Godovski, D.Y. *Adv. Polym. Sci.* 1995, *119*, 79.

8. An entire issue of "Chemistry of Materials" is devoted to 36 short reviews and 34 articles covering all aspects of nanocomposite hybrid inorganic-organic materials. *Chem. Mater.* 2001, *13*, 3059-3809.

9. Kickelbick, G. Prog. *Polym. Sci.* 2003, *28*, 83.

10. Lichtenhan, J.D. *Polymeric Materials Encyclopedia*, Salamone, J.C. Ed. CRC Press: New York, 1996, p.7769-7778.

11. Schwab, J.J.; Lichtenhan, J.D. *Appl. Organomet. Chem.*. 1998, *12*, 207.

12. Jeon, H.G.; Mather, P.T.; Haddad, T.S. *Polym. Inter.* 2000, *49*, 453.

13. Waddon, A.J.; Zheng, L.; Farris, R.J.; Coughlin, E.B. *Nano Lett.* 2002, *2*, 1149.

14. Haddad, T.S.; Viers, B.D.; Phillips, S.H. *J. Inorg. Organomet. Polym.* 2002, *11*, 155.

15. Fu, B.X.; Gelfer, M.Y.; Hsiao, B.S.; Phillips, S.; Viers, B.; Blanski, R.; Ruth, P. *Polymer* 2003, *44*, 1499.

16. Carroll, J.B.; Waddon, A.J.; Nakade, H.; Rotello, V.M. *Macromolecules* 2003, *36*, 6289.

17. Leu, C-M.; Chang, Y-T. Wei, K-H. *Chem. Mater.* 2003, *15*, 3721.

18. Leu, C-M.; Reddy, G.M.; Wei, K-H.; Shu, C-F. *Chem. Mater.* 2003, *15*, 2261.

19. Lichtenhan, J.D.; Otonari, Y.; Carr, M.J. *Macromolecules* 1995, *28*, 4355.

20. Haddad, T.S.; Lichtenhan, J.D. *Macromolecules*. 1996, *29*, 234.

21. Xu, H.; Kuo, S-W.; Lee, J-S.; Chang, F-C. *Polymer* 2002, *43*, 5117.

22. Xu, H.; Kuo, S-W.; Lee, J-S.; Chang, F-C. *Macromolecules* 2002, *35*, 8788.

23. Kim, K-M.; Keum, D-K.; Chujo, Y. *Macromolecules* 2003, *36*, 867.

24. Wright, M.E.; Schorzman, D.A.; Feher, F.J.; Jin, R-Z. *Chem. Mater.* 2003, *15*, 264.

25. Naka, K.; Itoh, H.; Chujo, Y. *Nano Lett.* 2002, *2*, 1183.

26. Feher, F.J.; Schwab, J.J.; Tellers, D.M.; Burstein, A. *Main Group Chem.* 1998, *2*, 123.

27. Li, G.; Wang, L.; Ni, H.; Pittman, Jr., C.U. J. *Inorg. Organomet. Polym.* 2002, *11*, 123.

28. Bowers, M.T.; Kemper, P.R.; von Helden, G.; van Koppen, P.A.M. *Science* 1993, *260*, 1446.

29. Clemmer, D.E.; Jarrold, M.F. *Mass Spectrom. Rev.* 1997, *32*, 577.

30. Hillenkamp, F.; Karas, M.; Beavis, R.C.; Chait, B.T. *Anal. Chem.* 1991, *63*, 1193A.

31. Lee, A.; Lichtenhan, J.D. *Macromolecules* 1998, *31*, 4970.

32. Lee, A.; Lichtenhan, J.D.; Reinerth, Sr., W.A. *Polym. Mater. Sci. Eng.* 2000, *82*, 235.

33. Baker, E.S.; Gidden, J.; Fee, D.P.; Kemper, P.R.; Anderson, S.E.; Bowers, M.T. *Int. J. Mass Spectrom.* 2003, *227*, 205.

34. Gidden, J.; Wyttenbach, T.; Batka, J.J.; Weis, P.; Jackson, A.T.; Scrivens, J.H.; Bowers, M.T. *J. Am. Soc. Mass Spectrom.* 1999, *10*, 883.

35. Gidden, J.; Bowers, M.T. *Eur. Phys. J. D* 2002, *20*, 409.

36. Gidden, J.; Bushnell, J.E.; Bowers, M.T. *J. Am. Chem. Soc.* 2001, *123*, 5610.

37. Jorgensen, W.J.; Severance, D.L. *J. Am. Chem. Soc.* 1990, *112*, 4768.

A home-built MALDI-TOF instrument was utilized in performing experimental analysis on the styryl/epoxy-POSS sample, which was synthesized by Dr. Rusty Blanski at the Air Force Research Laboratory. The details regarding the experimental setup for the mass spectrum and ion mobility measurements have previously been published[1], so only a brief description will be given. Sodiated styryl/epoxy-POSS ions were formed by MALDI in a home-built ion source. 2,5-dihydroxybenzoic acid (DHB) was used as the matrix and tetrahydrofuran (THF) as the solvent. Approximately 50 μL of DHB (100 mg/mL), 50 μL of the POSS sample (1 mg/mL) and 8 μL of NaI (saturated in THF) were applied to the sample target and dried. A nitrogen laser (λ=337 nm, 12 mW power) was used to generate ions, using MALDI methods, in a two-section (Wiley-McLauren) ion source. The ions were accelerated with 9kV of acceleration voltage down a 1-meter flight tube, while the TOF was operated in reflectron mode to obtain high-resolution mass spectra of the ions formed in the source.

In order to perform ion mobility experiments, the reflectron was turned off and an opposing voltage applied to the ions before the drift cell. This causes deceleration of the ions, which prevents collision-induced dissociation and allows the ions to be gently injected into the 20-cm long glass drift cell filled with ~1.5 torr of helium gas. By controlling the flow rate of warmed or cooled nitrogen through passages surrounding the drift cell, the temperature of the cell can be varied from 80K to 500K in order to meet the needs of the experiment. A weak, uniform electric field across the cell gently pulls the ions through the He gas at a constant drift velocity. After exiting the drift cell, the ions are gently accelerated through a quadrupole mass filter, which mass selects the ion of interest to be detected with an electron multiplier. The quadrupole is set to a specific mass-to-charge ratio (m/z) to eliminate any ions that might arise from fragmentation in the drift cell and interfere with the ion mobility experiments. The pulsed source extraction voltage triggers a timing sequence so that the ions are detected as a function of time, yielding an arrival time distribution or ATD. The reduced mobility, K_o, of the ion is accurately determined from a series of ATDs measured at different electric field strengths (7.5 –16

the drift cell. Through the use of kinetic theory the ion's collision cross-section can also be calculated.

Data Analysis. The reduced mobility of the mass-selected ions can be obtained from the ATD using Equation 1

$$K_o = \left(l^2 \cdot \frac{273}{760T} \cdot \frac{p}{V} \cdot \frac{1}{t_A - t_o} \right) \qquad (1)$$

where l is the length of the cell, T is the temperature in Kelvin, p is the pressure of the He gas (in torr), V is the strength of the electric field, t_A is the ions' arrival time taken from the center of the ATD peak and t_o is the amount of time the ion spends outside the drift cell before reaching the detector[2]. A series of arrival times (t_A) are measured by changing the voltage (V) applied to the drift cell. A plot of t_A vs. p/V yields a straight line with a slope inversely proportional to K_o and an intercept of t_o. Once K_o is found, the ion's collision cross-section can be obtained using Equation 2

$$\Omega^{(1,1)} = \frac{3e}{16N_o} \left(\frac{2\pi}{\mu k_b T} \right)^{1/2} \frac{1}{K_o} \qquad (2)$$

where e is the charge of the ion, N_o is the number density of He at STP, T is temperature, k_b is Boltzmann's constant and μ is the ion-He reduced mass[2].

Theoretical Modeling. By comparing the experimental cross-section from the ATDs to the cross-sections of theoretical structures, the conformation of the ion of interest can be analyzed. Molecular mechanics/dynamics methods are required to generate the trial structures for large molecules like this POSS system. We were able to parameterize the AMBER set of molecular mechanics/dynamics programs[3] to include silicon using published ab initio calculations by Sun and Rigby[4]. The parameters were tested for a number of POSS compounds with different Si-O cages and R substituents[1,5] and in

agreed well with known X-ray structures and ion mobility data.

Using the appropriate AMBER parameters, trial structures were calculated for $Na^+Sty_5Ep_3T_8$, $Na^+Sty_6Ep_2T_8$ and $Na^+Sty_7EpT_8$. An annealing/energy minimization cycle was used to generate 100 low-energy structures for each Sty/Ep combination. In this cycle, an initial minimization of the structure is followed by 30ps of molecular dynamics at 600K and 10ps of molecular dynamics in which the temperature is incrementally dropped to 0K. The resulting structure is then energy minimized again and used as the starting structure for the next minimization/dynamics run. After the low-energy structures (usually 100 to 200) are obtained, theoretical cross-sections must be calculated for comparison with experimental cross-sections. A temperature-dependent projection model[6,7] with appropriate atomic collision radii calculated from the ion–He interaction potential, is used to calculate the angle-averaged collision cross-section of each theoretical structure. A scatter plot of cross-section vs. energy is collected for the minimized structures and used to help identify the ions observed in the experimental ATDs. The average cross-section of the lowest 3-5 kcal/mol structures is used for comparison to experiment.

References:

1. Baker, E.S.; Gidden, J.; Fee, D.P.; Kemper, P.R.; Anderson, S.E.; Bowers, M.T. *Int. J. Mass Spectrom.* 2003, *227*, 205.

2. Mason, E.A.; McDaniel, E.W. *Transport Properties of Ions in Gases*, Wiley: New York, 1988.

3. Case, D.A.; Pearlman, D.A.; Caldwell, J.W.; Cheatham III, T.E.; Ross, W.S.; Simmerling, C.L.; Darden, T.A.; Merz, K.M.; Stanton, R.V.; Cheng, A.L.; Vincent, J.J.; Crowley, M.; Tsui, V.;

Singh, U.C.; Weiner, P.K.; Kollman, P.A. AMBER 6.0, 1999, University of California, San Francisco.

4. Sun, H.; Rigby, D. *Spectochim. Acta A* **1997**, *53*, 1301.

5. Gidden, J.; Kemper, P.R.; Shammel, E.; Fee, D.P.; Anderson, S.E.; Bowers, M.T. *Int. J. Mass Spectrom.* **2003**, *222*, 63.

6. von Helden, G.; Hsu, M.T.; Gotts, N.; Bowers, M.T. *J. Phys. Chem.* **1993**, *97*, 8182.

7. Wyttenbach, T.; von Helden, G.; Batka Jr., J.J.; Carlat, D.; Bowers, M.T. *J. Am. Soc. Mass Spectrom.* **1997**, *8*, 275.